Electromagnetically induced transparency of an interacting cold Rydberg ensemble

K J Weatherill, J D Pritchard, M G Bason, A K Mohapatra and C S Adams

Department of Physics, Durham University, Rochester Building, South Road, Durham DH1 3LE, UK

E-mail: `k.j.weatherill@durham.ac.uk`

Abstract. We study electromagnetically induced transparency (EIT) of a weakly interacting cold Rydberg gas. We show that for Rydberg states with principal quantum numbers in the range $n = 19 - 26$, the onset of interactions is manifest as a depopulation of the Rydberg state. In the limit of a weak probe where the depopulation effect is negligible, we observe no evidence of interaction induced decoherence and obtain a narrow Rydberg dark resonance with a linewidth of <600 kHz.

PACS numbers: 03.67.Lx, 32.80.Rm, 42.50.Gy

Ensembles of Rydberg atoms display fascinating many-body behavior due to their strong interactions [1]. These interactions lead to interesting cooperative effects such as superradiance [2, 3, 4] and dipole blockade [5, 6, 7, 8], which may provide the basis for applications such as single–photon sources [9] and quantum gates [10, 11, 12]. For quantum information applications one is interested in the coherent evolution of the ensemble. Coherent excitation of Rydberg states has been achieved using adiabatic passage [13, 14]. Rabi oscillations between ground and Rydberg states with dipole–dipole interactions have been observed [15, 16]. Also, the coherence of a Rydberg ensemble has been measured directly using a spin echo technique [17]. In most experiments on ultracold Rydberg gases, the Rydberg atoms are detected indirectly following field ionization and subsequent detection of electrons (or ions) using a micro channel plate (MCP). However, recently we demonstrated non-destructive optical detection of Rydberg states in room temperature Rb vapor [18, 19] using EIT [20, 21]. The same technique was subsequently used to detect Rydberg states in a Sr atomic beam [22]. Rydberg EIT has number of potential applications, for example, a Rydberg EIT medium displays a giant dc electro—optic effect many orders of magnitude larger than other systems [23] enabling precision electrometry, and Rydberg EIT could be used to a realize a photonic phase gate [24]. However, exactly how interaction effects are manifest in Rydberg EIT, e.g. as a dipole-dipole induced level shift, decoherence or loss is unknown.
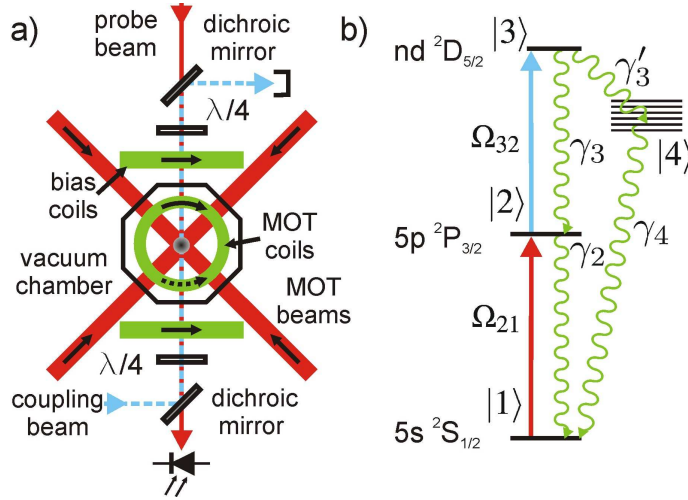
Figure 1. (Color online) (a) Schematic of the experimental setup. A strong coupling beam (blue) stabilized to the 5p ^{2}P$_{3/2}$ $\rightarrow$ nD (or nS) transition counter–propagates a weak probe beam (red) through a cold sample of ^{85}Rb released from a magneto–optical trap (MOT). The probe scans over a range of ± 20 MHz about the $F = 3 \rightarrow F' = 4$ resonance in 480 μs. (b) Simplified level scheme, Rabi frequencies and decay rates used to model the Rydberg EIT. Levels $|4\rangle$ represent states other than state $|2\rangle$ to which the Rydberg state $|3\rangle$ can decay.

In this work we demonstrate EIT involving Rydberg states in an ultra–cold atomic sample. We show that interactions between Rydberg atoms lead to a rapid depopulation of the Rydberg state, and that the EIT spectra are extremely sensitive to small changes in the interaction strength. For example, changing the principal quantum number of the Rydberg state from n to $n + 1$ produces a significant change in the EIT spectrum. By using a weak probe, where the probability of populating the Rydberg state is low, we can eliminate this depopulation effect and obtain narrow Rydberg dark resonances with a linewidth of $<$ 600 kHz.

The experimental setup and simplified level scheme are shown in figure 1 (a) and (b) respectively. A probe and coupling beam are combined using dichroic mirrors and counter–propagate through a cloud of laser–cooled ^{85}Rb atoms. The polarization of the beams are chosen to maximize transition strengths (σ^+–σ^+). The probe beam is derived from a diode laser at 780.24 nm stabilized to the $|1\rangle \rightarrow |2\rangle$, 5s ^{2}S$_{1/2}(F = 3)$ $\rightarrow$ 5p ^{2}P$_{3/2}$ ($F' = 4$) transition using polarization spectroscopy [25]. The frequency is controlled using two successive acousto-optic modulators (AOMs). The beam is then coupled into an optical fiber, the output of which is collimated and passed through an aperture resulting in a beam of almost uniform intensity and radius of 0.75 mm. The coupling beam is derived from a commercial frequency doubled diode laser system (Toptica TA-SHG) at λ=483–487 nm resonant with the $|2\rangle \rightarrow |3\rangle$, 5p ^{2}P$_{3/2}$ ($F' = 4$) $\rightarrow$ nd ^{2}D$_{5/2}$ (or ns ^{2}S$_{1/2}$) (F'') transition and passed through an optical fiber. The beam has a 1/e^2 radius of 0.8 mm and power up to 97 mW. The frequency of the coupling laser is stabilized using a Rydberg EIT signal produced in a magnetically shielded rubidium

vapor cell at room temperature [26].

We load approximately 10^8 atoms in a magneto–optical trap (MOT) in 5 s. A subsequent 10 ms optical molasses phase cools the atoms to a temperature of approximately 20 μK and density 10^{10} cm^{-3}, following which the cooling light is extinguished. An optical pumping pulse of variable duration prepares the atoms in the $F = 3, m_F = 3$ state. After 3 ms free expansion the coupling and probe beams are turned on and the frequency of the probe is swept across the D2 $F = 3 \rightarrow F' = 4$ transition. The sweep covers $\pm$ 20 MHz on either side of the resonance in 480 μs. Absorption measurements show that there is negligible density decrease over the duration of the scan and negligible optical pumping into the lower ($F = 2$) hyperfine ground state for the probe powers of interest. The probe beam is incident on a fast photodiode which records the transmission through the sample. This technique of measuring the narrow linewidth EIT spectra from a cold atomic sample within a single experimental cycle offers a faster repetition rate than ionization experiments. In addition Rydberg EIT provides a continuous probe of the Rydberg energy level with a bandwidth limited by the larger of the linewidth of the intermediate state or the two–photon Rabi frequency [23]. A disadvantage of Rydberg EIT is that one only obtains information about the population in the ground state and the coupled Rydberg state. In contrast, state-selective field ionisation techniques where the population in other Rydberg states can be detected is better suited to studying population transfer processes.

In figure 2 we show a series of EIT spectra for a fixed probe power of 3.6 μW corresponding to 0.13 I_{sat}, where I_{sat} is the saturation intensity on the $|1\rangle \rightarrow |2\rangle$ transition. The absorption data has been corrected for the measured change in probe intensity through the optical fiber as a function of AOM frequency. The effect of varying the cloud density, ρ, and principal quantum number, n, are shown in figures 2 (a) and (b), respectively. The density, ρ, is changed by heating the atom cloud (of initial density ρ_0) with the probe beam prior to the EIT scan. In figure 2 (b) the power of the coupling laser is varied to make the coupling Rabi frequency the same for each scan. For low ρ or low n a characteristic EIT spectrum is observed with a slight asymmetry. As ρ or n are increased this asymmetry becomes more pronounced until the transparency peak is lost completely. The lineshape for $n > 22$ does not change dramatically with n as illustrated by the similarity to the $n = 26$ and $n = 22$ data sets, the front curves in figure 2 (a) and (b), respectively. The data presented in figure 2 is suggestive of a density–dependent depopulation of the Rydberg state.

By varying the probe power we can change the fractional probability that an atom is excited to the Rydberg state. In figure 3 we show the transmission spectrum for the $|3\rangle$=19d state for two probe powers of 450 nW (0.016 I_{sat}) and 3.6 μW (0.13 I_{sat}). In this case we present double scans where the probe laser detuning is first increased and then decreased through the resonance in a total time of 960 μs. We observe that at the higher probe power there is significantly less absorption on the second scan than the first indicating that atoms excited to the Rydberg state are being lost from the EIT system. For these parameters only a small fraction of the population, a few percent, is transferred
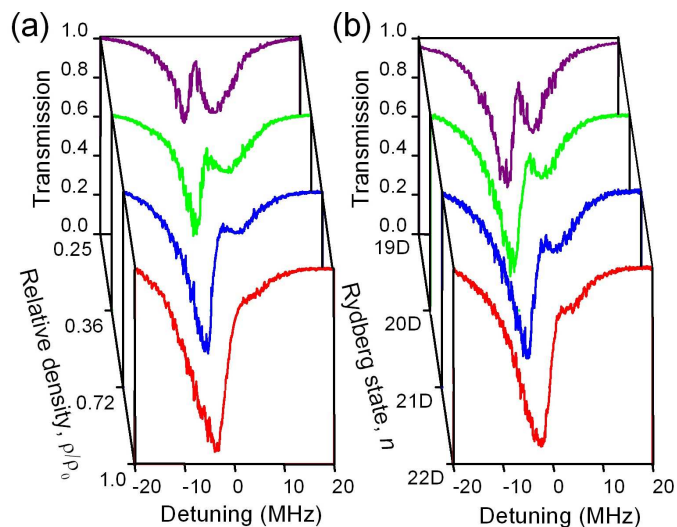
Figure 2. (Color online) (a) Transmission of a 3.6 μW probe beam as a function of probe laser detuning for the ^{85}Rb $|1\rangle \rightarrow |2\rangle \rightarrow |3\rangle = 26d$ system for varying atomic density. Constant coupling beam power of 97 mW (b) EIT spectra for n=19–22. The Rabi frequency of the $|2\rangle \rightarrow |3\rangle$ transition is kept the same for each state varying from 61 mW for $n = 19$ to 74 mW for $n = 22$. In both plots the onset of density–dependent behavior is evident in the emergence of an EIT lineshape at lower values of n and ρ

into and out of the Rydberg state for a time of order 10 μs. However, to model the data (see next paragraph) we find that >70% of the atoms are lost from the 3-level EIT system. This substantial loss cannot be explained by spontaneous decay from Rydberg state (since the spontaneous lifetime is also of order $\sim$10 μs [27] and decreases with larger n) or by optical pumping to the lower hyperfine state. We therefore deduce that there is an interaction induced loss from the system happening on a much faster time scale than the Rydberg state lifetime. In addition, with the available frequency resolution we are unable to resolve any dipole-dipole induced shift which is not unexpected for the Rydberg density and principal quantum numbers accessible in the current study.

To describe this interaction–induced depopulation we add non-linear density dependent decay and decoherence terms to the standard three-level optical Bloch equations [21]:

$$i\hbar\dot{\sigma} = [H, \sigma] - \gamma\sigma \tag{1}$$

where σ is the density matrix, H the atom-light interaction Hamiltonian and $\gamma\sigma$ the decoherence matrix. The depopulation of the Rydberg state is modeled by introducing a fourth level $|4\rangle$ to represent the reservoir of states other than $|2\rangle$ to which an atom in Rydberg state $|3\rangle$ could decay, as shown in figure 1 (b). The decay of the Rydberg state $|3\rangle$ is given by $\gamma_3\sigma_{33} + \gamma_3'\sigma_{33}^2$ where the first term is due to spontaneous emission and the second term is a density-dependent interaction induced loss to the reservoir states $|4\rangle$. The spontaneous decay rates of states $|2\rangle$ and $|3\rangle$ are given by γ_2 and γ_3, respectively. We assume that 50% of the spontaneous decay from $|3\rangle$ populates state $|2\rangle$ and 50% is lost

to the reservoir $|4\rangle$, however this weighting makes little difference to the lineshape as it is the non-linear term, γ'_3, that dominates. Atoms decay from $|4\rangle$ to $|1\rangle$ at a rate γ_4. The coherences are assumed to decay at half the rate of the populations. The decoherence rate between $|1\rangle$ and $|3\rangle$, γ_{31}, is included as a fitting parameter which depends on the combined laser linewidth and dephasing due to Rydberg atom interactions. The optical Bloch equations are then solved using a time varying probe detuning to match the experimental sequence. As the probe is swept through the two–photon resonance the Rydberg state is first populated and then depopulated by chirped adiabatic passage, in contrast to conventional adiabatic passage schemes where the transfer is unidirectional [13, 14]. The predictions of the model are compared to the experimental spectra in figure 3. The model accurately reproduces the observed spectra for different values of the probe laser intensity (all other parameters remain the same). When the probe intensity is increased the population of the Rydberg state (solid lines in the lower panel of figure 3) also increases and there is a faster decay into the reservoir states (dotted line in the lower panel of figure 3). For a higher probe power of 3.4 μW the model predicts that the maximum population of the coupled Rydberg state is only 2%, however, after the double scan sequence 76% of the population is in other states, $|4\rangle$.
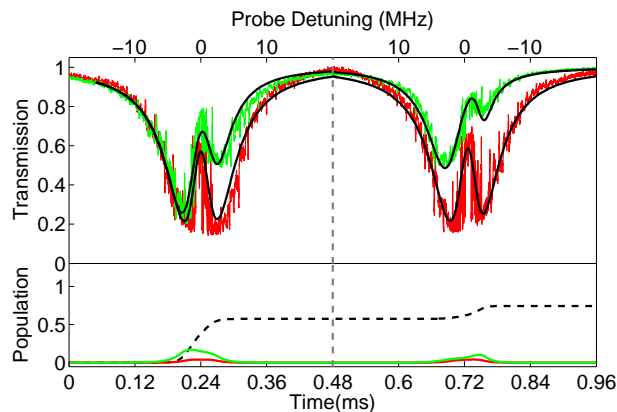

Figure 3. (Color online) Top: Double scan EIT for the $|1\rangle \rightarrow |2\rangle \rightarrow |3\rangle = 19$d system for probe powers of 450 nW (red) and 3.4 μW (green). The model fits are shown as the solid black lines. Bottom: The populations of the Rydberg states $|3\rangle$ ×25 (solid) and reservoir states $|4\rangle$ for the 3.4 μW probe scan (dashed) as a function of time during the scan. The parameters used in the fit are $\gamma_3 = 2\pi \cdot 21$ kHz and the peak value of $\gamma'_3 \sigma_{33} = 2\pi \cdot 216$ kHz and $2\pi \cdot 960$ kHz for the 450 nW and 3.4 μW scans respectively.

Although there is a number of possible mechanisms for the loss of Rydberg atoms from the system, eg. dipole-dipole energy transfer [28], the most likely conjecture for low n states is that the decay out of the EIT system is driven by superradiant decay of the Rydberg state to nearby f and p states. Observation of similar loss dynamics from nearby s states support this supposition as the dipole–dipole interactions are repulsive (attractive) for s (d) states [29]. The potential importance of superradiance in frozen

Rydberg gases particularly involving lower n states has been highlighted in recent work [4, 30]. In general superradiance is more significant for low n as the decay rate to nearby Rydberg levels scales as $1/n^5$, however there is also a geometrical effect which depends on the wavelength of the superradiant transition, λ_s, in comparison to the size of the cloud, D [30]. For the range of n studied in this work ($n = 19$ to 26) λ_s is less than D for decay to the closest f states i.e. the atoms are spatially spread over a range greater than the transition wavelength such that cooperative effects are small. However, λ_s is of order or greater than D for decay to the closest p states i.e. all atoms are within one wavelength and the emission rate is greatly enhanced. In this critical region the geometric cooperativity parameter [30] increases rapidly with increasing n which could explain the dramatic evolution of EIT spectra shown in figure 2 (b). The dependence of superradiance on λ_s and D is supported by the similarity of figure 2 (a) and (b) where for both data sets the value of $\lambda_\mathrm{s}D$ varies by a factor of 1.6 between the front and back trace [31]. Our simple non–linear optical Bloch equation model begins to fail for larger n. For example, for the high density 26d trace shown in figure 2 (a) no evidence of EIT is observable whereas the model predicts a pronounced shoulder after the laser has passed through the two–photon resonance. We also note that one can obtain a better fit to the high density and higher n data by coupling the optical Bloch equations to an equation describing the superradiance field energy density. This model reproduces the lineshapes observed in the experiment, in particular the complete loss of the EIT shoulder, however as the time scale of the decay of the superradiance field is not known, this model does not provide useful quantitative information. The current experimental arrangement precludes the unambiguous identification of the depopulation mechanism since neither ionized atoms or superradiant emissions (with wavelength in the range of 1 mm) can be detected directly. Further evidence could be obtained by performing experiments for a larger range of n, however, for the current geometry (approximately spherical excitation volume with diameter 1 mm) we are limited to $n \lesssim 26$ by the available coupling laser power (80 mW).

Of more interest to applications in non-linear optics [23], high resolution spectroscopy and electrometry is the weak probe limit where the population of the Rydberg state is small. This limit highlights the power of EIT as a non-destructive continuous probe of Rydberg states. Figure 4 shows the transmission spectrum for the $|3\rangle$=26d state using a low probe power of 200 nW (0.007 I_sat). In this case no loss or additional decoherence of the Rydberg state is observed between the forward and back scan. We obtain a typical EIT linewidth of 600 kHz. The EIT linewidth is made up of two terms; a term proportional to the coupling Rabi frequency squared, Ω_{32}^2 (i.e. the Autler–Townes splitting), and a term corresponding to the coherence between the ground state and the Rydberg state, γ_{31}. This coherence term is the sum of the combined laser linewidth and interaction dependent dephasing mechanisms. From the fit we obtain $\Omega_{32}/2\pi = 1.8\pm0.3$ MHz and $\gamma_{31} = 100\pm20$ kHz, i.e. for our parameters the linewidth is dominated by the Autler-Townes term. We observe no change in γ_{31} over the range $n = 19$ to $n = 26$ showing that the combined laser linewidth dominates over

any interaction induced dephasing of the Rydberg state. Note that such long coherence times cannot be observed in non–Rydberg cascade EIT due to the short lifetime of the upper state. The frequency resolution obtained using this method is comparable to the best obtained on single atoms [15] and considerably better than the resolution obtained for other ensembles experiments [16, 32, 33], where interaction effects tend to broaden the linewidth to greater than one MHz. This narrow resonance demonstrates a significant advantage of EIT for precision spectroscopy or electrometry, i.e. that the observed transparency is sensitive to the Rydberg energy level without transferring significant population into it. From the OBE model we find that the probability for an atom to be in the Rydberg state to be $\sim 0.15\%$ giving $\rho < 10^7$ cm^{-3} which corresponds to a total Rydberg population of less than 10^4 atoms.
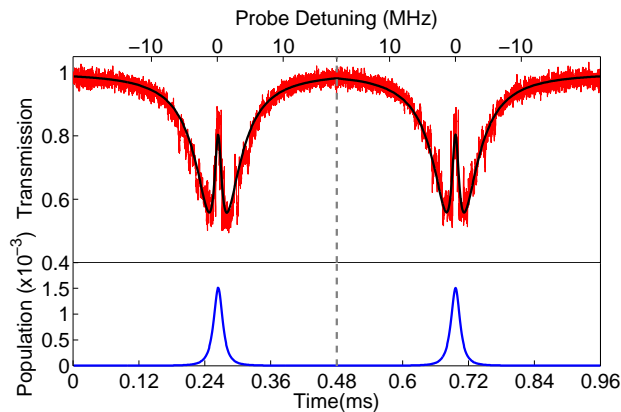

Figure 4. (Color online) Top: Double scan EIT for the $|1\rangle \to |2\rangle \to |3\rangle = 26d$ system with a probe power of 200 nW and coupling beam power of 60 mW. The solid line (black) is the theoretical line of best fit giving an EIT linewidth of 0.58 ± 0.04 MHz. Bottom: Population of the Rydberg state as a function of time for the duration of the scan.

In conclusion, we have shown that EIT is a useful technique to probe the properties of interacting Rydberg ensembles. We find that for principal quantum numbers in the range $n = 19-26$, interaction effects are manifest as a rapid depopulation of the Rydberg state. This density dependent loss can be modeled heuristically using non–linear optical Bloch equations. The character of the loss is similar for changes in either the atomic density or the principal quantum n of the Rydberg state, suggesting a superradiant decay mechanism. In the limit of weak probe power, where the depopulation effect is negligible we observe no evidence of interaction induced decoherence and the linewidth is limited by the Autler–Townes splitting. In this limit EIT provides a sensitive non–destructive probe of cold Rydberg ensembles. In contrast to conventional spectroscopy, Rydberg EIT allows one to probe Rydberg energy levels continuously without significant Rydberg population thereby interaction induced line broadening mechanisms can be controlled allowing high–resolution spectroscopy of Rydberg states. In future work we will focus

on extending the range of Rydberg EIT to smaller excitation volumes and states with higher principal quantum numbers, where dipole-dipole induced energy level shift are expected to dominate over superradiant decay.

References

[1] Gallagher T. F., 1994 *Rydberg atoms.* (Cambridge: Cambridge University Press).

[2] Gross M. and Haroche S., 1982 *Superradiance: An essay on the theory of collective spontaneous emission.* Phys. Rep., **93**, 301.

[3] Rehler N. E. and Eberly J. H., 1971, *Superradiance.* Phys. Rev. A. **3**, 1735.

[4] Wang T., Yelin S. F., Côté R., Eyler E. E., Farooqi S. M., Gould P. L., Koštrun M., Tong D. , and Vrinceanu D., 2007, *Superradiance in ultracold Rydberg gases.* Phys. Rev. A. **75**, 033802.

[5] Singer K., Reetz-Lamour M., Amthor T., Marcassa L. G., and Weidemüller M., 2004, *Suppression of excitation and spectral broadening induced by interactions in a cold gas of Rydberg atoms.* Phys. Rev. Lett. **93**, 163001.

[6] Tong D., Farooqi S. M., Stanojevic J., Krishnan S., Zhang Y. P., Côté R., Eyler E. E., and Gould P. L., 2004, *Local Blockade of Rydberg Excitation in an Ultracold Gas.* Phys. Rev. Lett. **93**, 063001.

[7] Cubel Liebisch T., Reinhard A., Berman P. R., and Raithel G., 2005, *Atom counting statistics in ensembles of interacting Rydberg atoms.* Phys. Rev. Lett. **95**, 253002.

[8] Heidemann R., Raitzsch U., Bendkowsky V., Butscher B., Löw R., Santos L., Pfau T., 2007, *Evidence for coherent collective Rydberg excitation in the strong blockade regime.* Phys. Rev. Lett. **99**, 163601.

[9] Saffman M. and Walker T. G., 2002, *Creating single-atom and single-photon sources from entangled atomic ensembles.* Phys. Rev. A. **66**, 065403.

[10] Jaksch D., Cirac J. I., Zoller P., Rolston S. L., Côté R. and Lukin M. D., 2000, *Fast quantum gates for neutral atoms.* Phys. Rev. Lett. **85**, 2208.

[11] Lukin M. D., Fleischhauer M., Côté R., Duan L. M., Jaksch D., Cirac J. I. and Zoller P., 2001, *Dipole blockade and quantum information processing in mesoscopic atomic ensembles.* Phys. Rev. Lett. **87**, 037901.

[12] Saffman M. and Walker T. G., 2005, *Entangling single- and N-atom qubits for fast quantum state detection and transmission.* Phys. Rev. A. **72**, 042302.

[13] Cubel T., Teo B. K., Malinovsky V. S., Guest J. R., Reinhard A., Knuffman B., Berman P. R., and Raithel G., 2005, *Coherent population transfer of ground-state atoms into Rydberg states.* Phys. Rev A **72**, 023405.

[14] Deiglmayr J., Reetz-Lamour M., Amthor T., Westermann S., de Oliveira A. L., and Weidemüller M., 2006, *Coherent excitation of Rydberg atoms in an ultracold gas.* Opt. Commun. **264**, 293.

[15] Johnson T. A., Urban E., Henage T., Isenhower L., Yavuz D. D., Walker T. G., and Saffman M., 2008, *Rabi oscillations between ground and Rydberg states with dipole-dipole atomic interactions.* Phys. Rev. Lett. **100**, 113003.

[16] Reetz-Lamour M., Deiglmayr J., Amthor T., and Weidemüller M., 2008, *Rabi oscillations between ground and Rydberg states and van der Waals blockade in a mesoscopic frozen Rydberg gas.* New J. Phys. **10**, 045026.

[17] Raitzsch U., Bendkowsky V., Heidemann R., Butscher B., Löw R., Pfau T., 2008, *Echo experiments in a strongly interacting Rydberg gas.* Phys. Rev. Lett. **100**, 013002.

[18] Mohapatra A. K., Jackson T. R., and Adams C. S., 2007, *Coherent optical detection of highly*

excited rydberg states using electromagnetically induced transparency. Phys. Rev. Lett. **98**, 113003.

[19] Bason M. G., Mohapatra A. K., Weatherill K. J., and Adams C. S., 2008, *Electro-optic control of atom-light interactions using Rydberg dark-state polaritons.* Phys. Rev. A. **77**, 032305.

[20] Boller K.-J., Imamoğlu A., and Harris S. E., 1991, *Observation of electromagnetically induced transparency.* Phys. Rev. Lett. **66**, 2593.

[21] Fleischhauer M., Imamoğlu A. and Marangos J. P., 2005, *Electromagnetically induced transparency: Optics in coherent media.* Rev. Mod. Phys. **77**, 633.

[22] Mauger S., Millen J. and Jones M. P. A., 2007, *Spectroscopy of strontium Rydberg states using electromagnetically induced transparency.* J. Phys. B. **40**, F319.

[23] Mohapatra A. K., Bason M. G., Butscher B., Weatherill K. J., and Adams C. S., 2008, arxiv.org/abs/0804.3273.

[24] Friedler I., Petrosyan D., Fleischhauer M., and Kurizki, G., 2005 *Long range interactions and entanglement of slow single-photon pulses.* Phys. Rev. A, **72,** 043803.

[25] Pearman C. P., Adams C. S., Cox S. G., Griffin P. F., Smith D. A., and Hughes I. G., 2002, *Polarization spectroscopy of a closed atomic transition: applications to laser frequency locking.* J. Phys. B **35**, 5141.

[26] Abel R. P., Mohapatra A. K., Bason M. G., Pritchard J. D., Weatherill K. J., and Adams C. S., 2008 *Laser stabilisation using electromagnetically induced transparency in a ladder system.* In preparation.

[27] Theodosiou C. E., 1984, *Lifetimes of alkali-metal atom Rydberg states.* Phys. Rev. A. **30**, 2881.

[28] Tanner P. J., Han J., Shuman E. S. and Gallagher T. F., 2008, *Many-body ionization in a frozen Rydberg gas.* Phys. Rev. Lett. **100**, 043002.

[29] Viteau M., Chotia A., Comparat D., Tate D. A., Gallagher T. F. and Pillet P., 2008, *Ionization in a frozen Rydberg gas with attractive or repulsive potentials* arXiv:0806.3402v1

[30] Day J. O., Brekke E., and Walker T. G., 2008, *Dynamics of low-density ultracold Rydberg gases.* Phys. Rev. A, **77**, 052712.

[31] In figure 2 (a) the density changes by a factor of 4 and hence the sample size D by a factor of $\sqrt[3]{4} = 1.58$ (with λ_s constant). In figure 2 (b) the cloud size and density remain constant but n changes from 19 to 22 and hence λ_s changes by a factor of $22^3/19^3 = 1.55$.

[32] Grabowski A., Heidemann R., Löw R., Stuhler J., and Pfau T., 2006, *High resolution Rydberg spectroscopy of ultracold Rubidium Atoms.* Fortschr. Phys. **54**, 765.

[33] Vogt T., Viteau M., Zhao J., Chotia A., Comparat D., and Pillet P., 2006, *Dipole blockade at Förster resonances in high resolution laser excitation of Rydberg states of cesium atoms.* Phys. Rev. Lett. **97**, 083003.